J. Opt. A: Pure Appl. Opt. **8** (2006) S330–S336 doi:10.1088/1464-4258/8/7/S06

A MEMS-based variable micro-lens system

F Krogmann, W Mönch and H Zappe

Department of Microsystems Engineering-IMTEK, University of Freiburg, Germany

E-mail: krogmann@imtek.de

Received 27 September 2005, accepted for publication 15 December 2005
Published 31 May 2006
Online at stacks.iop.org/JOptA/8/S330

Abstract
We present a tunable liquid micro-lens system exhibiting a tuning range of back focal length between 2.3 mm and infinity achieved by applying a voltage of 0–45 V. The lens actuation mechanism is based on electro-wetting on dielectrics (EWOD) and the system is fabricated in MEMS technology. In this system, two density-matched optical fluids are located in a centring structure which was defined by an anisotropic etching process. The system design provides an initial back focal length of a few millimetres and is robust against shocks and vibrations.

Keywords: electro-wetting, liquid lens, micro-lens, variable lens, optical fluids, micro-opto-electro-mechanical systems, silicon technology, centring structure

(Some figures in this article are in colour only in the electronic version)

1. Introduction

Tunable and adaptive optical components and systems have attracted increased attention in the field of applied optics during the past few years. However, the established means for the fabrication of tunable optical systems on a macroscopic scale cannot be continued on a microscopic scale. For microscopic tunable optical systems, new system designs and fabrication options have to be developed.

For sub-millimetre sizes, liquids are highly attractive for fabrication of micro-optical lenses because surface tension dominates over gravity at this length scale [1] and thereby highly precise spherical surfaces are formed naturally. Furthermore, the surface quality of liquids, showing a roughness of only a few nanometres, is advantageous for fabricating optical components. Currently, liquids for fabrication of optical components are used in several types of processes. For example, a well established process for the fabrication of micro-lens arrays is the photoresist reflow technique [2]: cylindrical photoresist posts, as defined by photolithography, are melted on a hot-plate or in an oven. In their liquid state, the photoresist posts take on a spherical shape under the influence of surface tension, forming micro-lenses. Usually, these photoresist micro-lenses are transferred into the substrate by appropriate etching processes.

Another way of exploiting the action of surface tension for the fabrication of micro-lens arrays is by patterning a glass substrate with hydrophobic and hydrophilic surface areas [3]. By selective adsorption of a photo-curable optical polymer on the circular domains, the polymer forms spherical caps which are subsequently cured by UV-light. Polymer micro-lenses fabricated using this process do not require an additional substrate transfer step.

Common to all these techniques is that the focal length is fixed after processing. To fabricate micro-lenses with an adjustable focal length, electro-wetting may be used to change the contact angle of a liquid droplet on a surface, thereby changing its curvature and thus tuning the focal length. Optical systems using this effect have been presented in [4] and [5] for use in cellular phone cameras in order to overcome the limitations of fixed focus lenses. Consequently, these systems are relatively large, with lens diameters of about 3 mm. These systems have the disadvantage that their fluids must be perfectly matched in their density and their density change due to temperature, because gravity plays a role for these diameters.

Other liquid lenses based on electro-wetting have also been presented [6]. It is, however, also a promising technique for numerous non-optical applications. It has been shown that transport, cutting and merging of liquid droplets [7] and the analysis of peptides and proteins [8], as well as the fabrication

1464-4258/06/070330+07$30.00

of light-wave coupled devices [9], benefit from application of this phenomenon.

In this work, we present a tunable liquid micro-lens system with a clear aperture between 300 and 800 μm. A highly parallel and reproducible process by using standard silicon MEMS processes has been developed for their manufacture. The systems presented here are very robust against environmental influences and achieved a focal length tuning range of 2.3 mm to infinity by application of a voltage of 0–45 V.

2. Theory

The micro-lens system presented in this work is based on a liquid lens which is actuated by electro-wetting. Under the action of surface tension, the shape of a liquid droplet resting on a planar substrate is a spherical cap. The contact angle of the liquid droplet on the substrate is given by the interfacial energies between the droplet and the ambient γ_{LG}, the liquid and the substrate γ_{SL}, and the substrate and the gaseous phase γ_{SG}. As surface tension dominates over gravity for water droplets with diameters of less than 1 mm, the effect of gravity on the shape may be neglected for small droplets [1]. The contact angle θ is given by the Young equation, namely

$$\gamma_{\mathrm{SL}} = \gamma_{\mathrm{SG}} - \gamma_{\mathrm{LG}} \cos(\theta). \tag{1}$$

When considering the liquid droplet as a plano-convex lens, the focal length of the lens is determined by the curvature of the surface of the droplet. We can thus calculate the back focal length, f, as a function of the contact angle,

$$f = \frac{d}{2\sin(\theta)(n-1)} \tag{2}$$

where d is the diameter of the lens and n the refractive index of the lens liquid.

Consequently, by changing the contact angle of the droplet, the focal length may be changed. A change in contact angle may be accomplished by introducing an additional energy term into the force balance described by the Young equation. Experimentally, this can be done by using a conductive substrate covered by an insulating layer and applying an electric voltage between the substrate and the droplet. The introduced electrostatic energy term, which is essentially the electric energy stored in a capacitor, causes the contact angle to decrease, i.e., the droplet spreads on the substrate.

This effect can be seen by inserting the electrostatic energy term into the Young equation, yielding the Lippmann equation

$$\cos(\theta) = \cos(\theta_0) + \frac{\epsilon\epsilon_0}{2\gamma_{\mathrm{LG}} d} V^2 \tag{3}$$

with V the voltage applied between substrate and droplet, d the thickness of the dielectric layer, θ_0 the initial contact angle and ϵ the dielectric constant of the dielectric layer.

This effect is called electro-wetting on dielectrics (EWOD). The effect itself was found by Lippmann in 1875 [10] upon observation of mercury drops in aqueous solutions.

As can be seen from equation (3), due to the quadratic dependence of the voltage, the polarity of the voltage is irrelevant, such that ac as well as dc voltages may be applied. Furthermore, the actuation voltage is a function of the thickness of the dielectric layer, implying that thinner surface layers will result in a decrease of the required actuation voltage.

3. Requirements for lens design

An electro-wetting based tunable micro-lens system must fulfil a number of requirements to yield a component whose performance is adequate for use in optical microsystems.

3.1. Positioning

The liquid lens has to be permanently centred in the optical axis of the system. Centring is necessary in order to prevent movement of the liquid out of the optical axis in the case of vibrations, mechanical shock or even actuation by electro-wetting. Centring may be accomplished by one of several techniques. One possibility is centring the lens by placing the drop in a recessed structure, e.g. holes or grooves. Surface defects may be used for forcing a pinning of the droplet to them.

Another approach is variation of the thickness of the dielectric layer. A thicker dielectric layer yields to a lower electric field and therefore to a higher contact angle. Therefore a ring of a thicker dielectric layer on the outside of the droplet forces the droplet to stay inside the ring whereas a disadvantage of this mechanism is that it only works while voltage is applied. Finally, a variation in the wettability of the substrate can centre drops. By having a hydrophilic spot on a hydrophobic substrate, a drop of liquid will stay in its initial position.

3.2. Liquid lens material

Liquid droplets are very sensitive to mechanical vibration or shock. These cause surface waves at the droplet/ambient interface and therefore introduce deviations from the intended spherical shape, thereby deteriorating the optical imaging properties. Shock and vibration sensitivity may be addressed by filling the system with a second, density-matched liquid, of lower refractive index than the lens liquid, and subsequently sealing the system hermetically. As an additional benefit, encapsulating the liquids also prevents their evaporation over time.

Control of the initial contact angle is a further issue that has to be addressed when choosing lens and surrounding liquids. By use of a conductive liquid with a high refractive index together with a non-conductive surrounding liquid with a low refractive index, the initial contact angle limits the minimal achievable focal length, since actuation of the droplet only allows movement toward smaller contact angles, i.e. towards higher focal lengths.

As a final consideration, a high difference in refractive indices between the two liquids is advantageous. If the system should provide a wide tuning range, and if the refractive index of the lens liquid is higher than that of the surrounding liquid, a high refractive index difference results in a low initial back focal length, which can then be increased by applying a voltage.

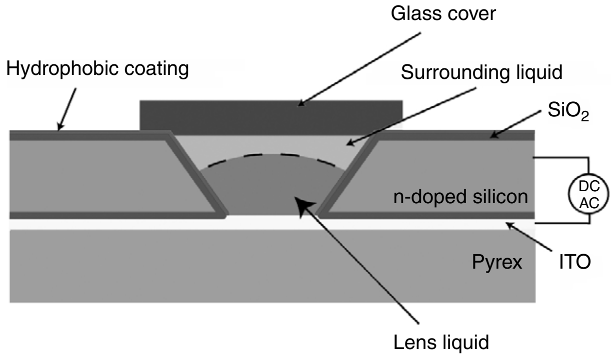

Figure 1. Schematic view of the tunable liquid micro-lens system. The liquid lens is positioned in a KOH-etched silicon groove, which is completely fabricated using MEMS processes. The remaining portion of the cavity volume is filled by a liquid immiscible with the liquid lens.

3.3. Electro-wetting actuation

As mentioned in section 2, the actuation principle for the liquid lenses is electro-wetting on dielectrics. For this actuation mechanism to work reliably, the dielectric layer should be free of defects and pinholes and exhibit a high dielectric strength. Otherwise, the capacitor may be shorted by defects leading to electrolysis and a slow self-destruction of the system. As can be seen from equation (3), low actuation voltages may be obtained by a reduced thickness of the dielectric layer.

To avoid pinning at surface defects during actuation, the surface roughness of the topmost layer must be low. Pinning of the liquid lens at defects would result in an undesired stick/slip motion upon actuation and in hysteresis during the tuning motion of the lens.

A last point to be considered in the design is electrical contacting of the droplet. Insertion of electrodes into the lens liquid must be avoided since this destroys the spherical shape by formation of a liquid capillary meniscus. For this reason, electrical contact must be achieved through the use of a flat conductive layer at the bottom of the lens liquid. We thus return the demands on the liquids employed: the lens material must have a high refractive index and be conducting, the surrounding liquid of lower refractive index while non-conducting and the two must have identical or closely matched densities.

4. System design

The system presented in this work is completely fabricated in MEMS technology. Starting with a standard silicon wafer, all the required features discussed above can be implemented, thus guaranteeing high stability of the system, a high reproducibility of the process and ultimately a compact, miniaturized lens which may easily fabricated in one- or two-dimensional arrays.

As shown in figure 1, the centring structure consists of quadratic V-groove-defined holes, which are formed inside a standard silicon wafer. All surfaces are covered with an insulating layer consisting of silicon dioxide and a hydrophobic layer. For contacting the droplet, an ITO-structured Pyrex wafer is anodically bonded to the bottom. The lens liquid is deposited in the middle of the V-groove, embedded in the surrounding liquid, and the system is closed by a glass cover.

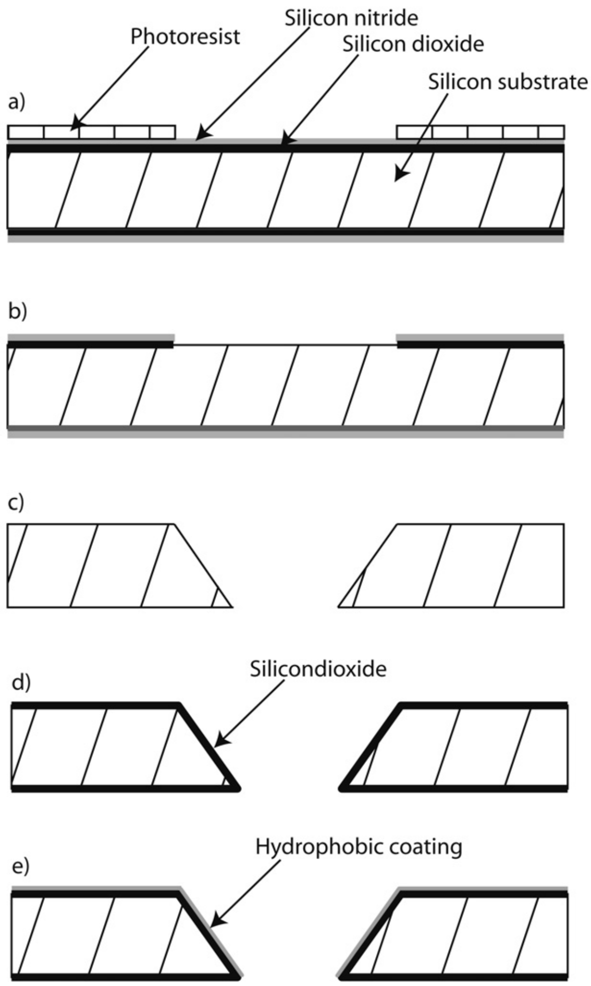

Figure 2. First part of the fabrication process: (a) Deposition of masking layers (silicon dioxide and silicon nitride); (b) structuring of the silicon nitride and silicon dioxide layer; (c) KOH etching and removal of the masking layer; (d) deposition of a thermally grown silicon dioxide layer; (e) deposition of a hydrophobic layer by using octafluorocyclobutane.

The lateral dimensions of system are 8 mm $\times$ 8 mm. Due to the use of 525 μm silicon wafers and 500 μm thick Pyrex wafers and the top glass, the total thickness of the system is 1.525 μm. The aperture of the lens, which is equivalent to the size of the bottom of the V-groove, was varied between 300 and 800 μm and the thickness of the dielectric layer was 300 nm.

No anti-reflection (AR) coating was deposited on the surfaces. These will be used in future work, and will result in an improvement of the efficiency. In any case, AR coatings are only required on the top and bottom surfaces of the device, due to the very low refractive index differences present in the system, making implementation of AR coatings straightforward and simple.

5. Fabrication

A summary of the fabrication process is shown in figures 2 and 3. The fabrication of the system is based on MEMS processes, so that high reproducibility and production accuracy

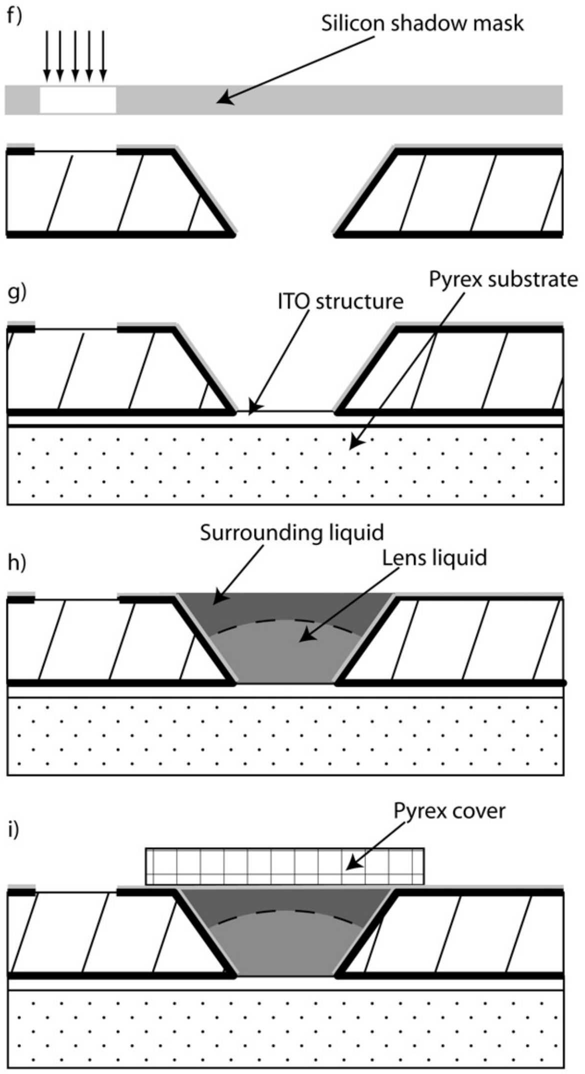

Figure 3. Second part of the fabrication process: (f) opening of the silicon dioxide layer by use of a shadow mask; (g) bonding an ITO-structured Pyrex substrate to the bottom of the substrate; (h) filling the device with surrounding and lens liquid; (i) closing the system with a top glass cover.

is achieved. Starting with a 4 inch, n-doped silicon wafer (100-orientation; thickness 525 μm; phosphorus doped; resistivity 1–5 Ω cm; polished on both sides), the silicon wafer is first covered with 300 nm thermally grown silicon dioxide and then 110 nm PECVD silicon nitride (see figure 2(a)). These silicon dioxide and nitride layers are lithographically structured with rectangular openings and act as a mask for the following etch step (figure 2(b)).

Etching is done by using 30% KOH aqueous solution at 80 °C for 7.7 h. Since, in KOH etching, the [100]-crystal facet is etched much faster than the [111], rectangular V-grooves with well defined sidewall angles of 54.7° are achieved. A low surface roughness between 60 and 100 nm for 30% KOH in aqueous solution [11] helps to avoid sticking effects and hysteresis. A well defined sidewall angle is necessary since this parameter directly enters the initial focal length.

After removing the silicon nitride and silicon dioxide etch stop layers (figure 2(c)), the substrate is again covered by a thermally grown silicon dioxide layer (figure 2(d)), which acts as the insulating layer between the droplet and the electrode. The advantages of thermal silicon oxide for electro-wetting applications are its high freedom of defects and pinholes, its high dielectric breakdown voltage, and its very uniform coverage of the V-groove [11]. Upon estimation of the voltage needed for a focal length of infinity and under consideration of the dielectric breakdown voltage, the necessary silicon dioxide thickness was determined to 300 nm.

In order to obtain a low initial focal length, the initial contact angle of the droplet on the side wall surfaces of the KOH groove has to be increased. One means to achieve a hydrophobic surface is the use of a perfluorocarbon coating, for example by coating the surface with Teflon AF (DuPont), which is frequently used in electro-wetting applications [12]. Teflon layers are usually processed by spin-coating or dip-coating from a solution onto the surface of interest. Unfortunately, these coating processes are not feasible in our design, due to the deeply structured features and the small edges in the surface topography.

An alternative approach is the use of the standard passivation layer of the so-called ‘Bosch’ dry-etch process. This dry-etch process yields high aspect ratios and a very directional etch by a repeated alternation between an etching step and a passivation step [11]. The passivation layer is deposited from gaseous C_4F_8 (octafluorocyclobutane) in a plasma process and yields a Teflon-like polymer (figure 2(e)). Using the passivation coating from this plasma process, we achieved a sufficiently high hydrophobicity of the surface with a contact angle to water of 96° and a highly reproducible quality of the surface properties. This layer was about 20 nm thick and was deposited in a STS Multiplex ICP system.

For electrical contacting of the silicon, the silicon dioxide layer on top of the silicon substrate was then partially opened by an RIE etch step using a shadow mask (figure 3(f)). Use of a shadow mask is necessary in this step since pattern definition using a standard photoresist-based lithography step is not possible due to the high aspect ratios of the KOH-etched structure.

For electrical contacting of the droplet, an ITO electrode structure on the Pyrex wafer was defined by photolithography. Afterwards, ITO from a target composed of 90 wt% In_2O_3 + 10 wt% SnO_2 was sputtered onto the Pyrex wafer in a DC-sputtering system at a pressure of about 2×10^{-2} mbar. Then, the ITO-covered wafer was annealed at 270 °C for 3 h in an oven.

The silicon and Pyrex wafers were then anodically bonded using a SUSS SB6 Vac Bonder (10 min at 1000 V, followed by 10 min at 2000 V, both at 280 °C) (figure 3(g)). After bonding, the wafers were diced.

The last step consisted of filling the structured wafers with the lens liquid and the surrounding liquid (figure 3(h)). The lens liquid was a water-based inorganic salt solution with a refractive index of 1.51 and a density of 2.1 g cm^{-3}. As a surrounding liquid, a density-matched perfluorocarbon with a refractive index of 1.293 was used. Finally, the system was closed by gluing using a Pyrex cover glass and a UV-curable adhesive on top of the liquid-filled groove (figure 3(i)).

The completed system can be seen in figure 4. The dimensions of this lens are 8 mm × 8 mm × 1.5 mm. The

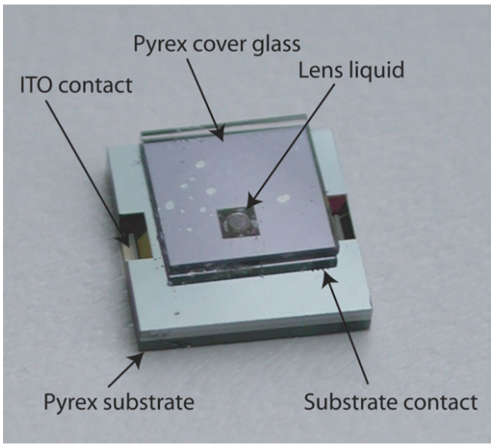

Figure 4. View of the completed silicon-based liquid lens system. Electrical contact to the droplet is achieved by the ITO contact shown on the left, and the silicon substrate is contacted by the opening shown on the right. Die size is 8 mm × 8 mm × 1.5 mm.

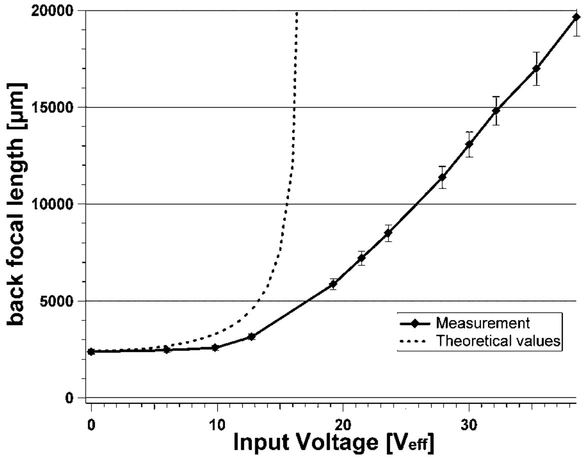

Figure 5. Measurement results of back focal length as a function of applied voltage for a system with an aperture of 300 μm and equal-density fluids. The theoretical curve is based on application of the Lippmann equation.

aperture of the lens, which is defined by the bottom opening of the V-shaped hole in the silicon wafer, was varied between 300 and 800 μm.

6. Measurement results

6.1. Measurement set-up

Focal length measurements of the system were performed using a Zeiss Axioplan 2, an optical microscope with a computer-controlled, motorized translation stage, in a set-up described in [3]: a collimated laser beam was transmitted through the lens from below, generating a focus spot above the lens system. The translation stage of the microscope was first moved such that the microscope is focused to the top of the device. Then, the translation stage was moved vertically to focus the microscope to the focal spot generated by the liquid lens system. The difference of z-positions of the translation stage corresponds to the back focal length of the liquid lens system.

The maximum measurable focal length with this set-up is 20 mm, due to the finite travel range of the motorized stage of the microscope. To verify that the focal length is infinity, the voltage on the lens was raised until the focal spot image created by the lens did not change upon moving the stage.

All measurements were made using 1 kHz AC driving voltage. The voltage was generated using a signal generator which controlled a high-voltage amplifier, similar to those used for driving piezo stacks. The voltage applied to the lens was measured and recorded using a voltmeter and the current was measured by an pico-ammeter.

6.2. Back focal length measurements

In figure 5, the back focal length as a function of the driving voltage for a system with an aperture of 300 μm is shown. The lens liquid volume was 100 nl with a tolerance of 10% and the initial contact angle was 96°. The initial back focal length, i.e. without an applied voltage, was 2.3 mm and, by applying a voltage of 45 V, the system reached a back focal length of infinity.

Theoretical values for focal length as a function of applied voltage were calculated using the Lippmann equation (3) for a two-dimensional cross section of the system. The discrepancy between the theoretical values and those of the measurement is due to two effects. First, the non-zero resistance of the ITO layer and the silicon reduces the electric field over the dielectric layer, which results in a higher threshold voltage than if these were ideal conductors.

Second, the resistance of the lens droplet results in a flattened characteristic and saturation in contact angle change. By decreasing the contact angle, the radius of the droplet increases and thus the distance between the ITO contact at the droplet and the liquid edges increases. Therefore, the voltage drop across the liquid increases and the electric field between the droplet and the electrode is reduced. A detailed description of the influences of this effect, including an even more flattened curve and contact angle saturation, is given in [13]. We are currently working on implementing our design in this model to obtain a better prediction of the behaviour of the lens.

6.3. Optical performance

For a first estimation of the optical performance, the surface of a droplet of lens liquid sitting in the V-groove was measured using a Zygo New View 5022 scanning white light interferometer (SWLI). The measurement was only possible without a surrounding liquid and the top glass cover, since sufficiently high reflectivity is required to perform this measurement. In the lens design, the surrounding liquid is used to avoid sticking of the lens liquid at the side walls and the top glass cover keeps away dust particles which cause sticking and deformation of the surface; therefore, insofar as optical quality of the surface is concerned, this represented the worst case scenario. As shown in figure 6, an area of 280 μm × 270 μm was measured; it was not possible to measure a larger area due to the finite numerical aperture of the SWLI objective lens. The aperture of the lens measured was 300 μm.

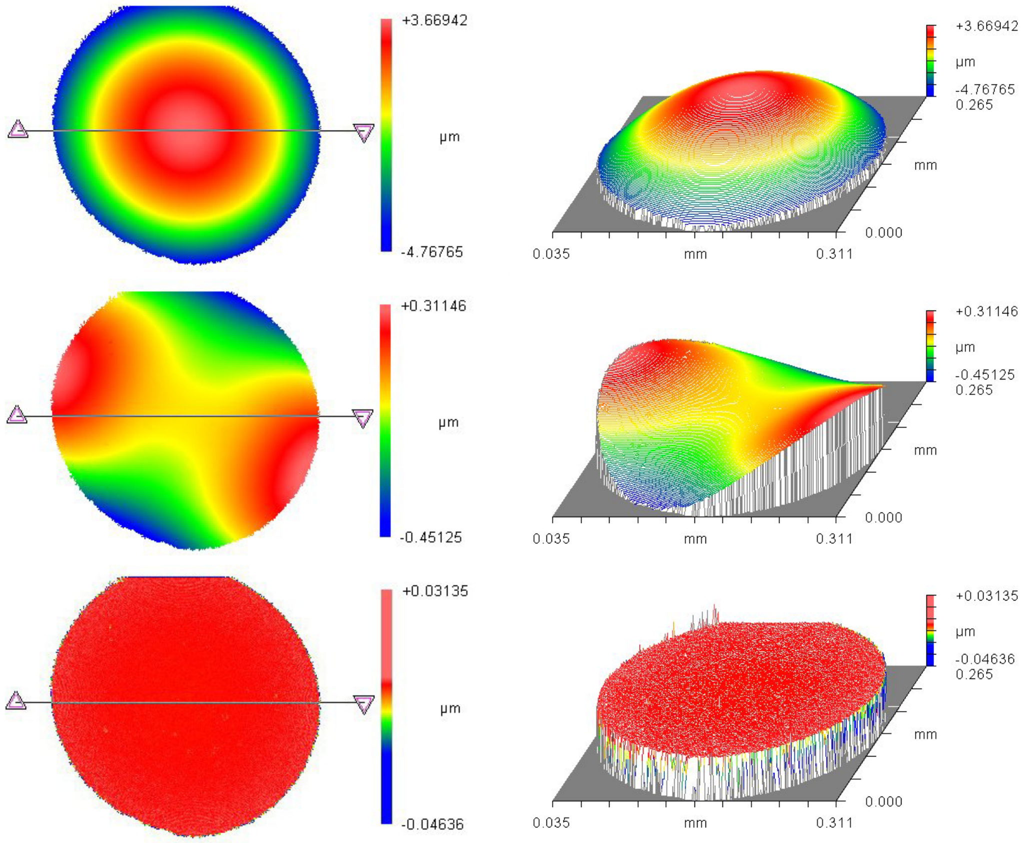

Figure 6. 2D (left) and 3D (right) plots of the surface of a liquid drop in a V-shaped centring structure measured using a white light interferometer. Top, a planar surface was numerically subtracted from the measured surface profile; middle, a spherical surface was numerically subtracted from the data to allow observation of the deviation of the lens from an ideal sphere; bottom, a high pass filter was used to eliminate the effects of the different radii of curvature.

By subtracting an ideal sphere from the measured surface profile, the deviation of the lens surface from this sphere may be plotted, as shown in the middle plots of figure 6. One can observe a saddle-point in the middle of the lens, caused by two different radii of curvature in the x- and y-directions. In total, a maximum peak-to-valley undulation of 763 nm is observed, due to sticking of the droplet on the sidewalls; this effect disappears when a surrounding liquid is employed. To obtain the roughness, a high pass filter was used to eliminate the effect of the different radii of curvature and the results can be seen in the bottom plot of figure 6; an rms roughness of 3 nm is found for the lens surface.

In figure 7 the focus spot of a lens with a aperture D of 400 μm is shown. The measurement set-up was the same as described in section 6.1. The focal length f of the system was 2.9 mm, and the wavelength λ was 546 nm. The distance between the maximum of the central spot and the first minimum of intensity is 4.01 μm. For a system limited by the diffraction of the bottom aperture, this latter value may be calculated by [14]

$$\frac{\lambda f}{D} = 3.96\ \mu\text{m} \tag{4}$$

showing that we are close to diffraction-limited performance for these lenses.

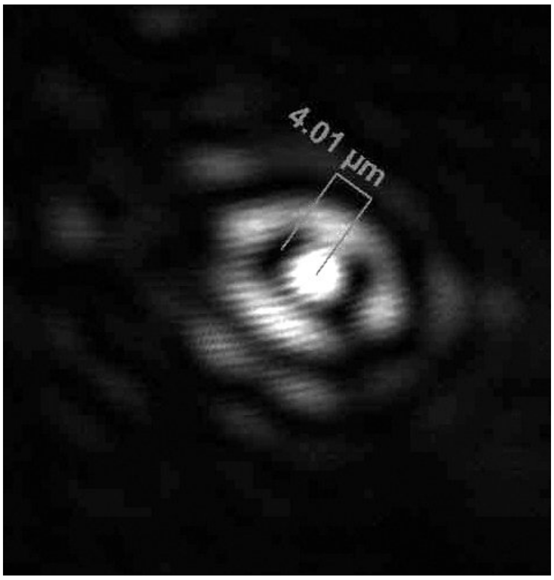

Figure 7. Focus spot of a collimated green laser beam focused through a lens with an aperture of 400 μm.

6.4. Power consumption

During actuation, the power consumption of the lens system was measured by monitoring the voltage required to drive the

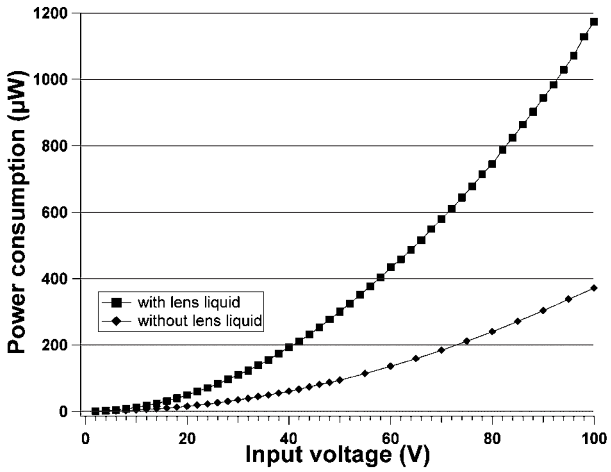

Figure 8. Power consumption of a lens with an aperture of 300 μm as a function of driving voltage, for the cases of presence and absence of lens liquid.

system, the leakage current which flows into the lens and the phase angle. By performing these measurements both with and without liquids in the V-groove, we were able to measure the power losses induced by the resistance of the silicon and the ITO as well as of the capacitances formed between the ITO wires and the substrate and the silicon itself. As shown in figure 8, the power consumption for maintaining a back focal length of infinity at a driving voltage of 45 V is about 0.3 mW. This value may be reduced by using an ITO layer of a higher conductivity and a silicon substrate of a lower electrical resistance.

7. Conclusion

A tunable micro-lens system based on electro-wetting and fabricated using MEMS technology has been presented. The back focal length can be varied between 2.3 mm and infinity by applying driving voltages of 0–45 V. Due to the use of two density-matched liquids and a hermetic seal, influences of vibration, mechanical shock or water evaporation were suppressed. Therefore, the system may be used in applications with significant mechanical movement, such as in endoscopy, handheld scanners or cell phone cameras. We have demonstrated that the use of silicon as a base material for fabrication of a variable lens system leads to advantages with respect to system properties such as actuation voltage, dielectric breakdown voltage, and surface roughness, and to a facilitated manufacturing process of the system.

Acknowledgment

We gratefully acknowledge financial support of the Landesstiftung Baden-Württemberg gGmbH.

References

[1] Landau L D and Lifshitz E M 1987 *Fluid Mechanics* vol 6 (Woburn, MA: Butterworth-Heinemann)
[2] Daly D 2000 *Micolens Arrays* (London: Taylor and Francis)
[3] Mönch W and Zappe H 2004 Fabrication and testing of micro-lens arrays by all-liquid techniques *J. Opt. A: Pure Appl. Opt.* **6** 330–7
[4] Berge B and Peseux J 2000 Variable focal lens controlled by an external voltage: an application of electro-wetting *Eur. Phys. J.* E **3** 159–63
[5] Kuiper S and Hendriks B H W 2004 Variable-focus liquid lens for miniature cameras *Appl. Phys. Lett.* **85** 1128–30
[6] Kwon S and Lee L P 2001 Focal length control by microfabricated planar electrodes-based liquid lens (μ-pell) *Proc. Transducers '01 Eurosensors XV (Munich, Germany, 10–14 June 2001)* pp 1348–51
[7] Cho S K, Moon H and Kim C-J 2003 Creating, transporting, cutting, and merging liquid droplets by electrowettinbg-based actuation for digital microfluidic circuits *J. Microelectromech. Syst.* **12** 70–80
[8] Wheeler A R, Moon H, Kim C-J, Loo J A and Garell R L 2004 Electrowetting-based microfluidics for analysis of peptides and proteins by matrix-assisted laser desorption/ionization mass spectroscopy *Anal. Chem.* **76** 4833–8
[9] Heikenfeld J and Steckl A J 2005 Intense switchable fluorescence in light wave coupled electrowetting devices *Appl. Phys. Lett.* **86** 011105
[10] Lippmann G 1875 Relations entre les phénomènes Électriques et capillaires *Ann. Chim. Phys.* **5** 494–549
[11] Madou M J 2002 *Fundamentals of Microfabrication* (Boca Raton, FL: CRC Press)
[12] Pollack M G, Shenderoc A D and Fair R B 2002 Electrowetting-based actuation of droplets for integrated microfluidics *Lab Chip* **2** 96–101
[13] Shapiro B, Moon H, Garrell R and Kim C-J 2003 Equilibrium behavior of sessile drops under surface tension, applied external fields and material variations *J. Appl. Phys.* **93** 5794–811
[14] Saleh B E A and Teich M C 1991 *Fundamentals of Photonics* (New York: Wiley)